19th Australasian Fluid Mechanics Conference
Melbourne, Australia
8-11 December 2014

Comparison between In-Flame and Exhaust Soot Particles in a Single-Cylinder, Light-Duty Diesel Engine

R. Zhang, Y. Zhang and S. Kook

School of Mechanical and Manufacturing Engineering
The University of New South Wales, NSW 2052, Australia

Abstract

Soot particle emissions from diesel engines are problematic due to its negative impact on human health and the environment. To help address this issue, we have studied morphological details of soot particles by implementing a direct in-flame soot sampling based on thermophoresis in a working diesel engine. This study further utilises this soot sampling technique and subsequent transmission electron microscope (TEM) imaging to compare in-flame and exhaust soot particles. Detailed analysis of TEM images reveal that both the soot particle concentration and primary particle size are significantly lower for the exhaust soot than those for the in-flame soot. This well expected trend is likely due to soot oxidation that occurred inside the engine cylinder before the particles exit through the exhaust. Also, it was found that the mean size and fractal dimension of soot aggregates are higher for the exhaust soot particles than those for the in-flame soot particles. This suggests that the compact aggregates are formed due to the soot burn-out occurring to the outer primary particles as well as in the linking primary particles with weaker oxidation resistant in large aggregates.

Introduction

Soot particle emissions from diesel engines raise health and environmental issues, primarily due to its micro and nano-scale sizes that can penetrate into human respiration systems [1]. Therefore, engine developers work towards new generations of diesel engines achieving low soot emissions. While the overall amount of soot particles have been reduced significantly, an outstanding issue is that soot particles emitted from current diesel engines have highly functionalized and defective surface structures [2]. Such structures can cause cytotoxic effects and stimulate inflammatory reaction much easier than those large soot particles from black-smoke diesel engines. Therefore, the need is clear for an improved understanding of soot particle size distribution and morphology.

Previous studies have provided information on tailpipe soot concentrations using commercially available instruments [3] or in-cylinder soot concentration using optical/laser based diagnostics [4]. Moreover, the engine-out soot sampling and morphology analysis using transmission electron microscope (TEM) have revealed morphology details of soot aggregates [5]. Our previous study further improved the soot sampling technique so that in-flame soot particles at high formation and oxidation stages can be collected in a working diesel engine [6]. The present study directly compares the exhaust soot particles and in-flame soot particles in the same engine and at fixed operating conditions. The thermophoretic soot sampling was conducted in a single-cylinder, small-bore diesel engine. The samples were imaged using a TEM. The images were then post-processed for statistical analysis of particle size distribution and fractal morphology.

Experiments

Single-Cylinder Optical Diesel Engine

An optically accessible, single-cylinder, small-bore diesel engine was used in this study. Detailed engine specifications and operating conditions are listed in table 1. Figure 1 shows the schematic diagram of the diesel engine and soot sampling system. A portion of the piston bowl-rim was removed to allow the insertion of a soot sampling probe into the combustion chamber without the risk of collisions with fast moving valves and piston. The compression ratio of the tested engine was 15.2 and the swirl ratio (mean flow speed over mean piston speed) was fixed at 1.4. Heated water at 90°C was supplied to the cylinder head and engine block to simulate warmed-up and stable engine conditions. Temperature of naturally aspirated intake air was measured at 30°C throughout the experiments. The engine speed was held constant at 1200 revolutions per minute (rpm) using a 37-kW AC motor. The engine was equipped with a second-generation Bosch common-rail system and a solenoid injector which were controlled by a universal engine control unit (Zenobalti 5100). The fuel used in the present study was ultra-low-sulphur diesel with cetane number of 51. The original nozzle tip had 7 holes with 134 μm nominal diameter. In this study, the six holes were laser-welded to create a single fuel jet that is isolated from complex jet-jet interactions. The single-hole approach also allowed for a long injection duration that corresponds to upper-mid to high load conditions where soot particle emissions are particularly problematic. The fuel mass per injection was 9 mg at injection duration of 2.34 ms (actual) and injection pressure of 70 MPa. The injection timing was set at -7°CA after the top dead centre (aTDC). The in-cylinder

Displacement volume	498 cc
Bore / Stroke	83 mm / 92 mm
Compression ratio	15.2
Swirl ratio	1.4
Coolant temperature	90℃
Intake air temperature	30℃
Engine speed	1200 rpm
Injection system	Bosch second-generation common-rail injector
Fuel	Ultra-low-sulphur diesel
Cetane number	51
Nozzle hole diameter	134 μm (nominal)
Mass per injection	9 mg
Injection pressure	70 MPa
Injection timing	-7 °CA aTDC

Table 1. Engine specifications and operating conditions.

combustion conditions were monitored by recording in-cylinder pressure traces using a piezoelectric pressure transducer (Kistler 6065A).

Soot Particle Sampling

As illustrated in figure 1, the single-hole was oriented such that the sooting diesel flame penetrated into the bow-rim cut-out region. At the tip of the sampling probe placed in this region, a 3-mm diameter, 400-mesh, carbon-coated TEM grid was attached. The grid was exposed to a sooting diesel flame inducing a high temperature gradient between hot soot-laden gas and cold carbon layer, which triggered the thermophoresis (i.e., positive thermal diffusion) and thus led to soot deposition on the grid. The soot reactions would freeze immediately, which preserves the original soot morphology [7]. A similar sampling method was used for exhaust soot collection. For this experiment, a sampling probe holding a TEM grid was inserted into the exhaust pipe right downstream of the exhaust manifold. The sampling probes used in this study were installed at a fixed location, meaning that the sampled soot particles would not represent those at any instant moment but rather a time-integrated result. However, due to short injection event and combustion occurring inside the engine cylinder, the in-flame soot exposure time to the TEM grid was 1~3 ms, which was similar to other thermophoretic sampling experiments conducted in open flame burners using a quick insertion-type probe [7]. Since much lower soot concentration was expected in the exhaust than inside engine cylinder [3], in-flame and exhaust soot particles were collected separately with different number of fuel injection cycles (5 cycles for in-flame soot and 20 for exhaust) to collect enough number of soot particles for statistical analysis [8].

Soot Particle Imaging and Image Post-Processing

A JEOL 1400 TEM unit with a point resolution of 0.38 nm and an acceleration voltage of 100 kV was used to perform imaging of the sampled soot particles. A CCD camera with a resolution of 11 mega pixels was used to digitise magnified soot particle images. Multiple images were taken from different locations on the TEM grid considering the variations in soot deposition. The magnification was set at ×50,000. The obtained TEM images were then post-processed using an in-house-developed Matlab code, which yielded the size distribution of both soot aggregates and primary particles. This information was then used to determine the fractal morphology of soot aggregates. Details of the image post-processing and calculations of the soot fractal morphology are found in our previous papers [6, 8].

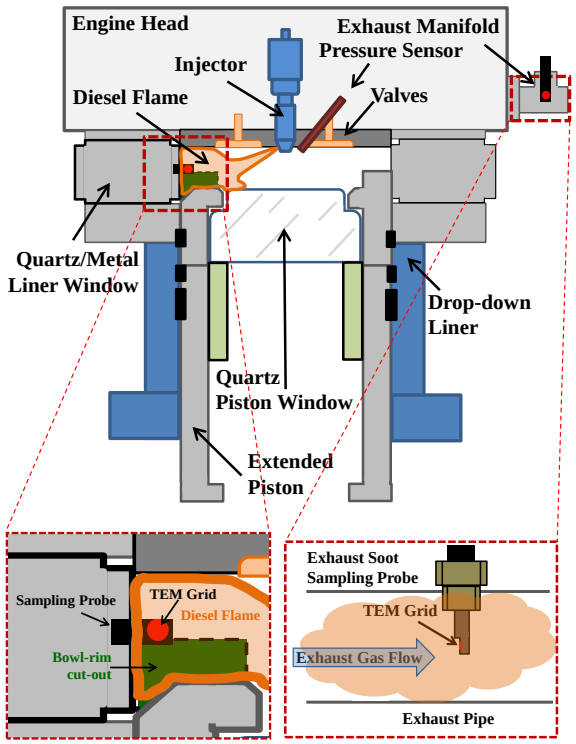

Figure 1. Cross-sectional view of the diesel engine (top) and the close-up views of the soot sampling regions (bottom).

Results and Discussions

Combustion Conditions

To ensure that the in-flame and exhaust soot sampling were conducted at the same combustion conditions, the in-cylinder pressure traces were measured, which was ensemble averaged and then used to calculate the apparent heat release rate (aHRR). The results are plotted for various crank angle locations in figure 2. The averaged pressure over 30 motoring cycles is also shown in the figure. The figure displays that the in-cylinder pressure traces of the in-flame and exhaust sampling experiments follow the motored pressure very well, prior to the start of injection at -7°CA aTDC. Afterwards, both traces show lower values than that of the motored cycle, evidencing the evaporative cooling of diesel fuel. The start of combustion is observed at around 9°CA aTDC as the in-cylinder pressure exceeds the motoring pressure. The aHRR traces show consistent trends with the in-cylinder pressure traces. The figure shows that differences in the in-cylinder pressure and aHRR traces are well within the cyclic dispersion and thus unlikely impact the soot particles [8].

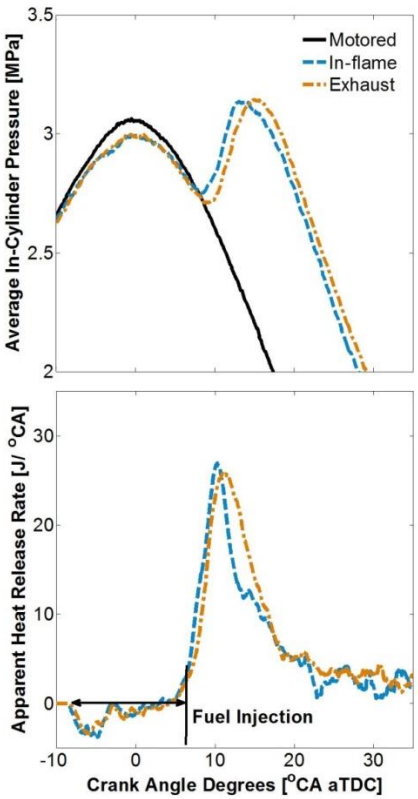

Figure 2. Averaged in-cylinder pressure and corresponding apparent heat release rate traces for various crank angle locations.

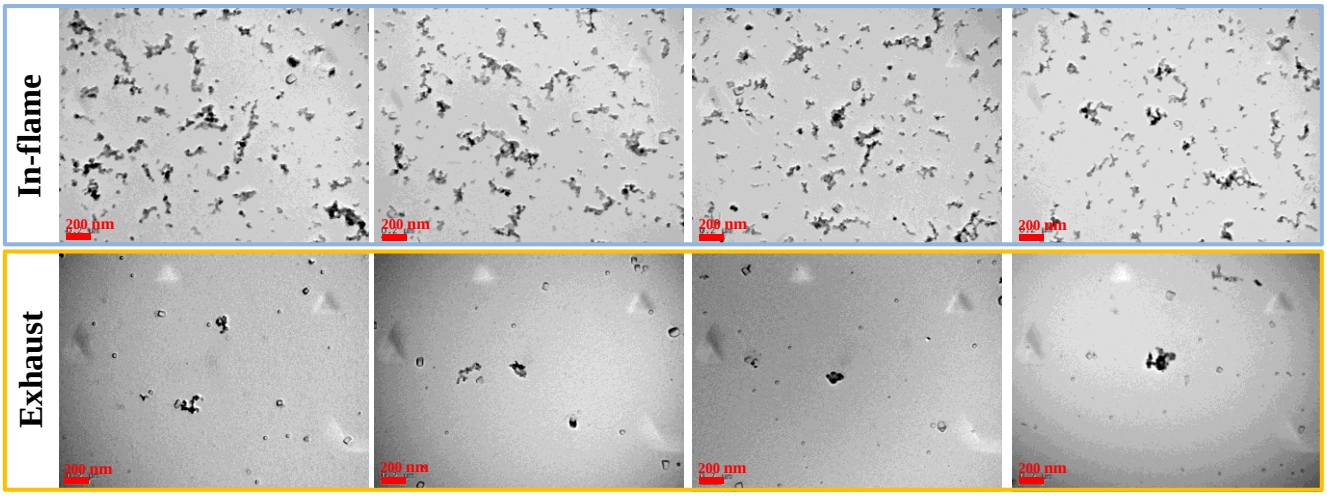

Figure 3. Example TEM images of soot particles. The scale bars of 200 nm are shown as red horizontal bars in the bottom-left corner of each image.

TEM Images

Figure 3 shows example TEM images for in-flame and exhaust soot particles. It is observed that the majority of sampled soot particles show solid carbon particle structures with fractal-like aggregate morphology. The aggregates appear to consist of many near-spherical primary particles. As expected, the particle number concentration decreases drastically for the exhaust sample, despite four-fold higher fuel injections. This is consistent with the observation of previous studies reporting that only a very small fraction of soot particles can survive the in-cylinder oxidation before they exit through the exhaust [3, 9]. A noticeable difference between the in-flame and exhaust samples is their morphology. For example, the in-flame soot particles show a mix of aggregates with various sizes and structures. Large aggregates (larger than the 200-nm scale bar) with chain-like branches are seen together with small aggregates comprised of only a couple of primary particles. Single-primary particles are also observed. On the other hand, the exhaust soot particles show less number of small particles and more compact aggregate structures. An interesting observation from most of the exhaust soot images and some in-flame soot images are the existence of crystalline-like objects with transparent appearance, which is presumed to be solidified, gas-phase combustion products other than soot particles [10].

Soot Particle Size Distribution

Soot particle size was quantified by measuring the radius of gyration (R_g) of soot aggregates as well as the diameter of primary particles (d_p). A total number of 1143 soot aggregates and more than 12,000 primary particles were processed to calculate the probability density function (pdf) of both R_g and d_p. The results are plotted in figure 4.

Figure 4 (top) shows that the mean R_g for the in-flame and exhaust soot aggregates are about 26 nm and 37 nm, respectively. From the pdf curves, a likely cause for the higher R_g of the exhaust soot is significantly reduced small (< 50 nm) aggregates. It was conceivable that most of small aggregates evident in the in-flame soot images (figure 3) were completely oxidized. For large aggregates, it was also thought that the primary particles in the outer branch and linking primary particles were oxidized first, resulting in compact aggregates with highly-concentrated primary particles.

Figure 4 (bottom) compares the pdfs of primary particle sizes between the in-flame and exhaust soot particles. It is observed that the mean d_p of the exhaust particles (15 nm) is 25% lower than that of the in-flame soot particles (20 nm). The reduction of

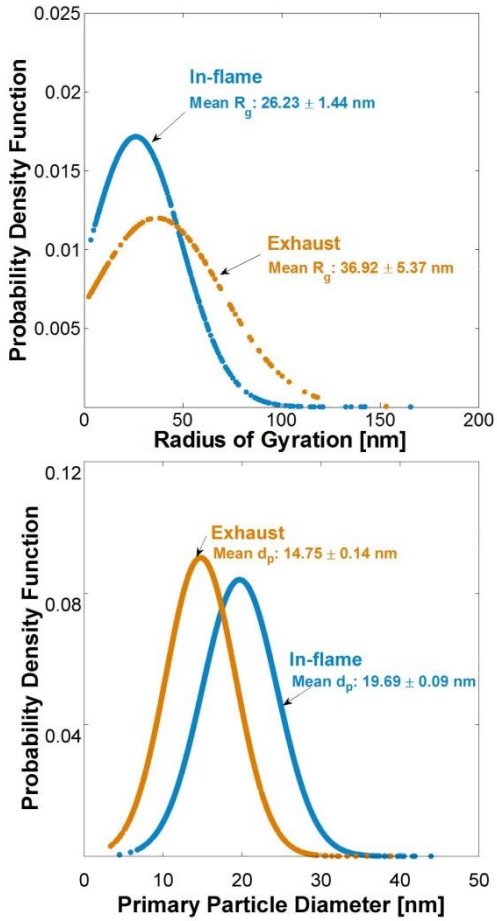

Figure 4. Probability density function of the radius of gyration (R_g) of soot aggregates (top) and the primary particle diameter (d_p) for in-flame and exhaust soot particles. The mean value and error range (95% confidence) are annotated.

the mean d_p suggests intense oxidation at primary particle levels, which occurred inside the engine cylinder.

Fractal Morphology of Soot Aggregates

The fractal morphology of soot aggregates is quantified by the fractal dimension (D_f) and prefactor (k_f) that are calculated using the number of primary particles (N), R_g and mean primary

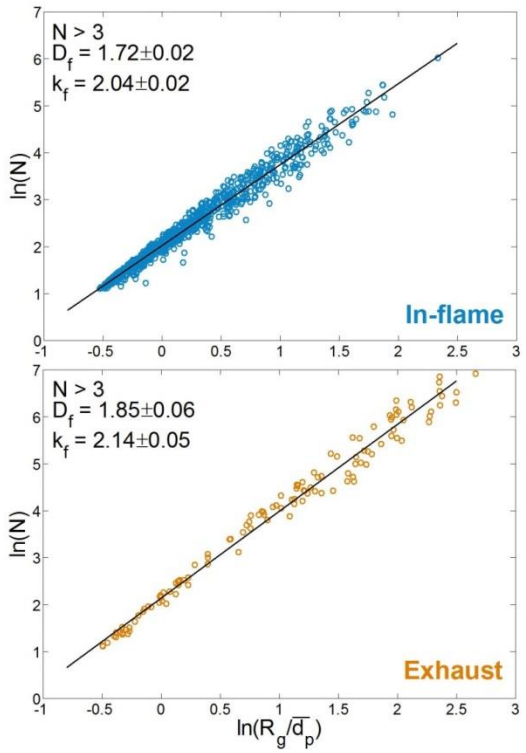

Figure 5. Statistical determination of soot aggregate fractal dimension (D_f) and prefactors (k_f) using the number of primary particles (N), radius of gyration (R_g) and mean primary particle diameter of each soot aggregate ($\overline{d_p}$). Error ranges were estimated with 95% confidence.

particle diameter ($\overline{d_p}$) of each soot aggregate. It should be noted that only those aggregate with more than three primary particles (N>3) were considered as fractals excluding monomers and dimers.

Figure 5 shows that the exhaust soot aggregates have higher D_f than the in-flame soot particles, suggesting more compact soot aggregates in the exhaust. One study [11] suggested that in-cylinder soot aggregates would have higher D_f due to the late-cycle oxidation, which is consistent with the results of the present study.

Conclusions

A thermophoretic soot particles sampling was conducted for in-cylinder diesel flame as well as the exhaust stream in a small-bore diesel engine. Soot samples were imaged using a transmission electron microscope and then post-processed for statistical analysis of soot particle size and fractal dimension. Major findings from this study are summarised as follows:

1) For the tested conditions of this study, the exhaust soot particles have much lower concentration than the in-flame soot particles.

2) The exhaust soot aggregates have higher mean radius of gyration than the in-flame soot aggregates as a result of the reduced number of aggregates that are smaller than 50 nm, due to soot oxidation.

3) The primary particle diameter of the exhaust soot particles is also lower than the in-flame soot particles, suggesting the intense oxidation at primary particle levels.

4) The fractal dimension of the exhaust soot particles is higher than the in-flame soot particles likely because small soot aggregates are completely oxidized and large aggregates undergo oxidation from the primary particles in outer and linking branches. This results in compact soot aggregates with highly-concentrated primary particles.

Acknowledgments

Experiments were conducted at the UNSW Engine Research Laboratory, Sydney, Australia. Support for this research was provided by the Australian Research Council via Discovery Project.

References

[1] Frank, B., Schlögl, R. & Su, D.S., Diesel Soot Toxification, *Environ. Sci. Technol*.,**47**, 2013, 3026-3027.

[2] Su, D.S., Serafino, A., Muller, J., Jentoft, R.E., Schlögl, R. & Fiorito, S., Cytotoxicity and Inflammatory Potential of Soot Particles of Low-Emission Diesel Engines, *Environ. Sci. Technol*.,**42**, 2008, 1761-1765.

[3] Pungs, A., Pischinger, S. & Bäcker, H., Analysis of the Particle Size Distribution in the Cylinder of a Common Rail DI Diesel Engine during Comubstion and Expansion, SAE Technical Papers, 2000-01-1999, 2000.

[4] Mathews, W.S., Fang, T., Coverdill, R.E., Lee, C.F. & White, R.A., Soot Diagnostics Using Laser-Induced Incandescence within an Optically Accessible HSDI Diesel Engine, SAE Technical Papers, 2004-01-1412, 2004.

[5] Neer, A. & Koylu, U.O., Effect of Operating Conditions on the Size, Morphology, and Concentration of Submicrometer Particulates Emitted from a Diesel Engine, *Combust. Flame*,**146**, 2006, 142-154.

[6] Zhang, R. & Kook, S., Influence of Fuel Injection Timing and Pressure on In-Flame Soot Particles in an Automotive-Size Diesel Engine, *Environ. Sci. Technol*.,**48**, 2014, 8243-8250.

[7] Dobbins, R.A. & Megaridis, C.M., Morphology of Flame-Generated Soot as Determined by Thermophoretic Sampling, *Langmuir*,**3**, 1987, 254-259.

[8] Kook, S., Zhang, R., Szeto, K., Pickett, L.M. & Aizawa, T., In-Flame Soot Sampling and Particle Analysis in a Diesel Engine, *SAE Int. J. Fuels Lubr*.,**6**, 2013, 80-97.

[9] Kunte, S., Bertola, A., Obrecht, P. & Boulouchos, K., Temporal Soot Evolution and Diesel Engine Combustion: Influence of Fuel Composition, Injection Parameters, and Exhaust Gas Recirculation, *Int. J. Engine Res.*,**7**, 2006, 459-470.

[10] Tree, D.R. & Svensson, K.I., Soot Processes in Compression Ignition Engines, *Prog. Energ. Combust.*,**33**, 2007, 272-309.

[11] Li, Z., Song, C., Song, J., Lv, G., Dong, S., & Zhao, Z., Evolution of the Nanostructure, Fractal Dimension and Size of In-Cylinder Soot during Diesel Combustion Process, *Combust. Flame*,**158**, 2011, 1624-1630.